

# Self-Assembly of Delocalized $\pi$ -Stacks in Solution. Assessment of Structural Effects

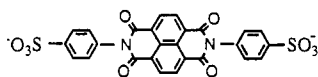
Chuan Jian Zhong, Wing Sum V. Kwan, and Larry L. Miller\*

Department of Chemistry, University of Minnesota, Minneapolis, Minnesota 55455

Received August 4, 1992. Revised Manuscript Received September 29, 1992

Twelve derivatives of 1,4,5,8-naphthalenetetracarboxylic acid diimide were prepared which had cationic, anionic, or neutral substituents on the nitrogens. These imides were characterized spectroscopically and studied using cyclic voltammetry. Reduction with dithionite in water produced anion radicals, which were studied with visible, near-IR, and ESR spectroscopy. It is shown that the anion radicals self-assemble into  $\pi$ -dimers and  $\pi$ -stacks. The stacks are characterized by exciton bands at wavelengths greater than 1200 nm and by anisotropic ESR signals. The effect of the substituents attached to nitrogen on the extent of aggregation is explored. Most effective are cationic groups which act to balance the charge on the aromatic anion radical. The relationship of these observations to conducting stacks in solid materials is discussed.

Mixed valence  $\pi$ -stacks containing ion radicals are found in a wide variety of single-crystal and polymeric synthetic metals.<sup>1</sup> Indeed, these delocalized stacks are the conducting entities in such materials. Recently, it has been reported from this laboratory that the imide anion radical  $1^-$  self-assembles in aqueous NaCl solutions to form  $\pi$ -



1

stacks.<sup>2</sup> Although  $\pi$ -dimers of ion radicals are well-known in solution,<sup>3</sup> the further aggregation to form organized supramolecular entities is not.<sup>4</sup> Since these stacks have electrons delocalized intermolecularly, they have unusual electronic properties. This is signified in particular by their optical spectra, which show absorption bands in the near-infrared (NIR) region that correspond to the "optical conduction bands"<sup>5</sup> of conducting solids. Thus, we are able to assemble the entities that are responsible for macroscopic conductivity in a dilute liquid phase.

In a related study from this laboratory it has been shown that coprecipitation of these stacks with a polymeric polycation forms a conducting polymer with very unusual properties.<sup>6</sup> Most important and unexpected is the high structural and conductance anisotropy of this material. We believe that the precipitation of preassembled stacks is important to achieving this anisotropic structure. Therefore, further study of these organized solution-phase assemblies is of importance, not only as a way to study the electronic properties of individual stacks in solution but

also because they are useful for preparative materials chemistry.

Some details of the observations and interpretations made for anion radical  $1^-$  are important here. In DMF solution  $1^-$  is monomeric, showing ESR with hyperfine coupling and visible spectra, both of which are in agreement with MO calculations. Essential to this project are the unusual solubility and stability of the naphthalene diimide anion radicals in aqueous media. In water,  $1^-$  forms a  $\pi$ -dimer, which is ESR silent and which shows a new absorption band at 1140 nm in the NIR. This band is the so-called charge-transfer (CT) band between the two  $1^-$  entities that comprise the dimer. The  $\pi$ - $\pi^*$  band is shifted from 473 nm in DMF to 451 nm in water. As the concentration of  $1^-$  in water is raised or NaCl is added, the NIR band maximum shifts to a longer wavelength, eventually reaching 1800 nm. The ESR spectrum is then anisotropic, because of slow rotation of the aggregated species. The  $\pi$ - $\pi^*$  band is now shifted to 439 nm. Solid samples of  $1^-$ , which are semiconducting, show similar spectra, and it is concluded that  $\pi$ -stacks are formed in these solutions. Analogy has also been drawn to  $\pi$ -aggregates of diamagnetic dyes, which show similar shifts in their visible spectra and similar salt and solvent effects.<sup>7</sup> In agreement with theory, these aggregates sometimes show excitonic bands but not optical conduction bands beyond 1000 nm.

The general idea of this stacking process for  $1^-$  is described in Figure 1, which also shows how  $\pi$ -dimerization provides stabilization and spin pairing. Stack formation provides further electronic stabilization by this mechanism. It is noted though that odd-membered stacks may be ESR active.

In the present study we explored the scope of this phenomenon for a number of naphthalenetetracarboxylic acid diimides **2** with different groups attached to the nitrogens. The simple diimide with hydrogens on the two nitrogens is designated **2(H)**.

## Results and Discussion

**Synthesis.** The compounds **2** were prepared in one or two steps from 1,4,5,8-naphthalenetetracarboxylic acid dianhydride and the appropriate amine.<sup>8</sup> The products were characterized by NMR, UV, visible, and IR spec-

(1) (a) Ferraro, J. R.; Williams, J. M. *Introduction to Synthetic Electrical Conductors*; Academic Press: New York, 1987. (b) Skotheim, T. A., Ed. *Handbook of Conducting Polymers*; Dekker: New York, 1986; Vols. 1, 2.

(2) Penneau, J.-F.; Stallman, B. J.; Kasai, P. H.; Miller, L. L. *Chem. Mater.* 1991, 3, 791.

(3) (a) Soos, Z. G.; Bondeson, S. R. In *Extended Linear Chain Compounds*; Miller, J. S., Ed.; Plenum Press: New York, 1983; pp 193-257. Nakayama, S.; Suzuki, K. *Bull. Chem. Soc. Jpn.* 1973, 46, 3694. de Sörgo, M.; Wasserman, B.; Szwarc, M. *J. Phys. Chem.* 1972, 76, 3468. Sakai, N.; Shirota, I.; Minomura, S. *Bull. Chem. Soc. Jpn.* 1971, 44, 675. (b) Ito, M.; Sasaki, H.; Takahashi, M. *J. Phys. Chem.* 1987, 91, 3932. Kimura, K.; Yamada, H.; Tsubomura, H. *J. Chem. Phys.* 1968, 48, 440. Evans, J. C.; Evans, A. G.; Nouri-Sorkhabi, N. H.; Obaid, A. Y.; Rowlands, C. C. *J. Chem. Soc., Perkin Trans.* 1985, 315. Wolszczak, M.; Stradowski, C. *Radiat. Phys. Chem.* 1989, 33, 355. Evans, A. G.; Evans, J. C.; Baker, M. W. *J. Am. Chem. Soc.* 1977, 99, 5882. (c) Boyd, R. H.; Phillips, W. D. *J. Chem. Phys.* 1965, 43, 2927.

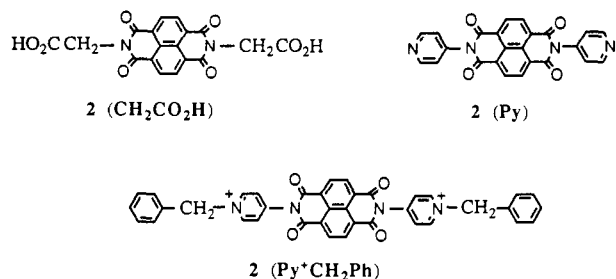
(4) Saeva, F. D.; Reynolds, G. A.; Kaszczuk, L. *J. Am. Chem. Soc.* 1982, 104, 3524.

(5) Torrance, J. B.; Scott, B. A.; Welber, B.; Kaufman, F. B.; Seiden, P. E. *Phys. Rev. B* 1979, 19, 730.

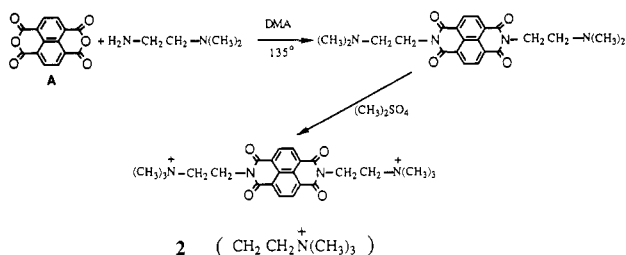
(6) Zhong, C. J.; Zinger, B.; Cammarata, V.; Kasai, P. H.; Miller, L. L. *Chem. Mater.* 1991, 3, 787.

(7) (a) Duff, D. J.; Giles, C. H. In *Water: A Comprehensive Treatise*; Franks, F., Ed.; Plenum Press: New York, 1975; Vol. 4, Chapter 3. (b) Herz, A. H. *Photogr. Sci. Eng.* 1974, 18, 323. (c) Kasha, M.; In DiBartolo, B. *Spectroscopy of the Excited State*; Plenum Press: New York, 1976.

(8) Dietz, T. M.; Stallman, B. J.; Kwan, W. S. V.; Penneau, J.-F.; Miller, L. L. *J. Chem. Soc., Chem. Commun.* 1990, 367.



troscopies and were specifically free from starting material or the intermediate amide acid. In many cases HPLC analysis was performed and confirmed the purity. The two-step process to form  $2(\text{CH}_2\text{CH}_2\text{N}^+\text{Me}_3)$  is shown in eq 1. The compounds  $2(\text{H})$ ,  $2(\text{OMe})$ ,  $2(\text{OH})$ , and  $2((\text{CH}_2)_5\text{CO}_2\text{H})$  were not water soluble, but the anion radicals could be formed by chemical reduction in aqueous solution in all cases.



**Cyclic Voltammetry (CV).** In DMF using either  $\text{Bu}_4\text{NBF}_4$  or  $\text{LiClO}_4$  each compound **2** showed two reversible couples (cathodic-anodic peaks separated by 60–70 mV, independent of sweep rate) separated by 300–500 mV.<sup>8</sup> Apparent  $E^\circ$  values (Table I) were taken as the center of the anodic and cathodic peak potentials, measured with respect to SCE, and are consistent with those reported for other aromatic imides.<sup>9</sup> Compounds **2** with cationic groups had first reduction potentials at more positive potentials, ca. –0.3 V, and anionic groups made the potentials more negative, ca. –0.6 V, effects that are expected based on Coulombic considerations.

It has been reported that **1** has two reversible couples in aqueous 0.1 M NaCl.<sup>2</sup> Three other anionically terminated **2** (the two sulfonates and the carboxylate in pH 7 solution) behave similarly (Table I). Although the processes are not perfectly reversible in the sense that the peak separation for the first reduction is not 60 mV in every case, the processes are chemically reversible. Shown in Figure 2 is the CV of  $2(\text{CH}_2\text{CO}_2^-)$  which shows a “prewave” at pH 7. At pH 10 this prewave is absent. The separation between the two reduction  $E^\circ$  values is in each case about 200 mV. The cationically substituted compounds **2** gave voltammograms in which the first reduction process was reversible, but there was only an ill-defined second reduction (Figure 2). With one exception, compound  $2(\text{Py}^+\text{CH}_2\text{Ph})$ , the second and later sweeps gave the same shape as the first sweep. In the case of  $2(\text{Py}^+\text{CH}_2\text{Ph})$  a noticeable precipitation of reduced material onto the electrode was noted, and the second and subsequent sweeps were quite distorted. Stirring the solution caused the precipitate to dissolve. It is proposed that the aggregation of the anion radicals is greater for these cationically substituted compounds and that this aggregation distorts the voltammograms. The reversibility of the first reduction suggests that on the CV time scale the aggregation is rapid and reversible. The second process may be distorted because of the formation of mixed aggregates

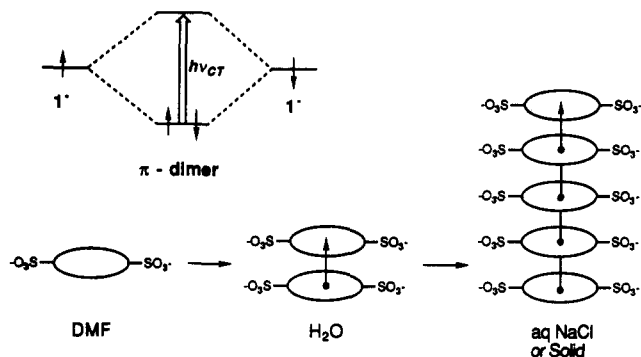


**Figure 1.** Schematic of  $\pi$ -dimerization and  $\pi$ -stacking. Perturbation diagram showing mixing of  $\pi$ -orbitals to form new  $\pi$ -orbitals of  $\pi$ -dimer.

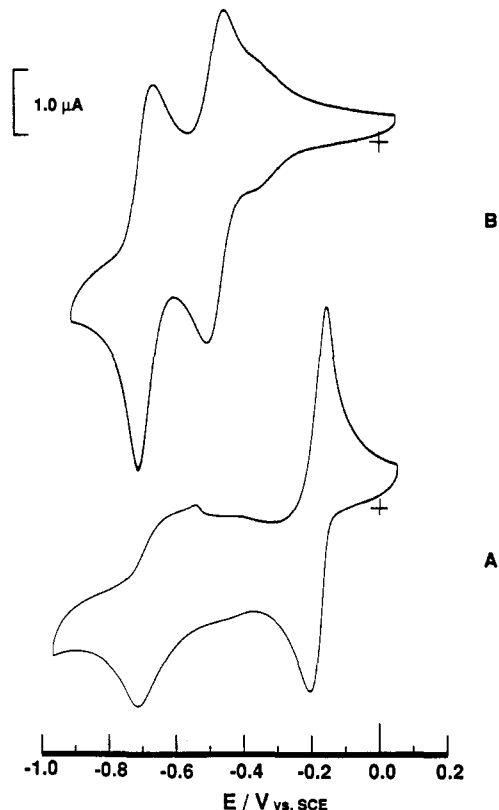


**Figure 2.** CV of (A)  $2(\text{Py}^+\text{Me})$  (1 mM) in aq 0.1 M NaCl; (B)  $2(\text{CH}_2\text{CO}_2\text{H})$  (1 mM) in aq 0.05 M pH 7 buffer. Sweep rate 10  $\text{mV s}^{-1}$ .

**Table I.** Reduction Potentials for **2**

cmpd	DMF/0.1 M $\text{Bu}_4\text{NBF}_4$		$\text{H}_2\text{O}/0.1 \text{ M NaCl}$	
	$-E_1^\circ$ (V)	$-E_2^\circ$ (V)	$-E_1^\circ$ (V)	$-E_2^\circ$ (V)
1	0.52	1.04	0.42	0.65
$2(\text{CH}_2\text{SO}_3^-)$	0.57	0.86 <sup>b</sup>	0.48	0.67
$2((\text{CH}_2)_3\text{SO}_3^-)$	0.52	1.01	0.45 <sup>b</sup>	0.67
$2(\text{CH}_2\text{CO}_2\text{H})$	0.48	0.90	0.48 <sup>c</sup>	0.68 <sup>c</sup>
$2(\text{Py}^+\text{Me})$	0.29	0.74	0.18	
$2(\text{Py}^+\text{CH}_2\text{Ph})$	0.30 <sup>a</sup>	0.76 <sup>a,b</sup>	0.14	
$2(\text{CH}_2)_2\text{N}^+(\text{Me})_3$	0.38	0.80	0.28	
$2(\text{CH}_2)_3\text{N}^+(\text{Me})_3$	0.45 <sup>a</sup>	0.86 <sup>a</sup>	0.33	0.65
$2(\text{H})$	0.54	0.98	<i>d</i>	<i>d</i>
$2(\text{OMe})$	0.39	0.86	<i>d</i>	<i>d</i>
$2(\text{Py})$	0.43	0.83	0.39 <sup>c</sup>	0.66 <sup>c</sup>

<sup>a</sup> DMF/0.1 M  $\text{LiClO}_4$ . <sup>b</sup>  $\Delta E_p > 0.06 \text{ V}$ . <sup>c</sup> 50% DMF–50%  $\text{H}_2\text{O}$  as solvent. <sup>d</sup> Not soluble in water. <sup>e</sup> pH 7 buffer as solvent.

of anion radical and dianion (see below).

**Vis-NIR Spectroscopy.** Spectra were recorded from 300 to 2600 nm. In DMF solution the vis spectra of the

Table II. Visible and NIR Bands of  $2^-$  in Aqueous Solutions

anion radical	$\lambda_{\max}/\text{nm}$	$\lambda_{\max}/\text{nm}$ ( $\Delta\lambda$ , eV) <sup>a</sup>
$1^-$	451	1140 (0.32)
$2^-(\text{CH}_2\text{SO}_3^-)$	449	1120 (0.31)
$2^-((\text{CH}_2)_3\text{SO}_3^-)$	450	1113 (0.33)
$2^-(\text{CH}_2\text{CO}_2\text{H})^b$	450	1112 (0.29)
$2^-((\text{CH}_2)_5\text{CO}_2\text{H})^b$	451	1117 (0.30)
$2^-(\text{Py}^+\text{Me})$	443	1700 (0.37)
$2^-(\text{Py}^+\text{CH}_2\text{Ph})$	442	2050 (0.29)
$2^-((\text{CH}_2)_2\text{N}^+(\text{Me})_3)$	447	1550 (0.42)
$2^-((\text{CH}_2)_3\text{N}^+(\text{Me})_3)$	449	1340 (0.42)
$2^-(\text{H})$	440	2200 (>0.5)
$2^-(\text{OMe})$	445	1291 (0.39)
$2^-(\text{Py})^b$	448	1400 (0.38)

<sup>a</sup> Peak width at half-height. <sup>b</sup> pH 7 buffer.

neutral compounds **2** had  $\lambda_{\max}$  380 ( $\epsilon$  14 000) and 360 ( $\epsilon$  13 000) nm. Anion radicals  $2^-$  in DMF showed  $\lambda_{\max}$  470  $\pm$  2 nm ( $\epsilon$  25 000) as well as weaker peaks near 604, 690, and 760 nm. This demonstrates that the substituent groups have virtually no effect on the electronic structure of the aromatic anion radical. Calculations<sup>10</sup> and ESR (see below) show there is little delocalization of the odd electron onto these groups, and so this is the expected result.

It has been shown for  $1^-$  that in DMF/water mixtures only  $\pi$ -dimers, not  $\pi$ -stacks, are formed.<sup>2</sup> Studied in DMF/water mixtures all the anion radicals  $2^-$  had  $\lambda_{\max}$  in the vis region at 451  $\pm$  2 nm and  $\lambda_{\max}$  in the NIR at 1130  $\pm$  10 nm. It is concluded that dimers were present in each case. As shown in Figure 1, bringing two anion radicals together in  $\pi$ -fashion perturbs the  $\pi$ -orbitals and allows the two originally unpaired electrons to go into a lower energy orbital. The CT transition is a measure of the strength of this perturbation. Therefore, the constancy of the  $\lambda_{\max}$  indicates that the substituent groups do not affect the strength of the  $\pi$ -bonding.

In water the anion radicals were formed using 1.1 equiv of the reducing agent sodium dithionite. When required by the structure of the substituent group, a small concentration (50 mM) of buffer was used to ensure the state of protonation. It is known that higher concentrations of  $1^-$  or added salt causes the anion radical  $1^-$  to aggregate more,<sup>2</sup> so the concentration of  $2^-$  was held constant at 0.9 mM and the buffer concentration was minimized. In Table II are recorded the  $2^-$   $\lambda_{\max}$  values for the strongest visible ( $\pi$ - $\pi^*$ ) peak and the NIR (dimer CT or stack exciton) peak. The presence of more than one aggregated species often gave NIR spectra which were unsymmetrical and broad. Therefore, the band width is also indicated in the table. Representative spectra are shown in Figure 3.

In contrast to  $1^-$ , which forms dimers (1140 nm) in water, the cationically substituted anion radicals show absorbances at longer wavelengths. These result from excitonic transitions and are characteristic of the formation of  $\pi$ -stacks.<sup>1-3</sup> The best stack formers were  $2^-(\text{Py}^+\text{Me})$  (1700 nm) and  $2^-(\text{Py}^+\text{CH}_2\text{Ph})$  (2050 nm). Also showing  $\pi$ -stack absorbances were  $2^-((\text{CH}_2)_2\text{N}^+(\text{Me})_3)$  (1550 nm) and  $2^-((\text{CH}_2)_3\text{N}^+(\text{Me})_3)$  (1360 nm) anion radicals. Comparing these  $\lambda_{\max}$  values indicates that in water with no added electrolyte all the cationically substituted compounds stack better than  $1^-$ . This is confirmed by the  $\lambda_{\max}$  values in the visible region. Shifts in the visible  $\pi$ - $\pi^*$  band maxima are interpreted by analogy to dye aggregation in solution.<sup>7</sup> It is known that diamagnetic, ionic dyes, e.g., cyanines, form stacked aggregates in aqueous media. Because stacking requires ions of the same charge to come together, it is

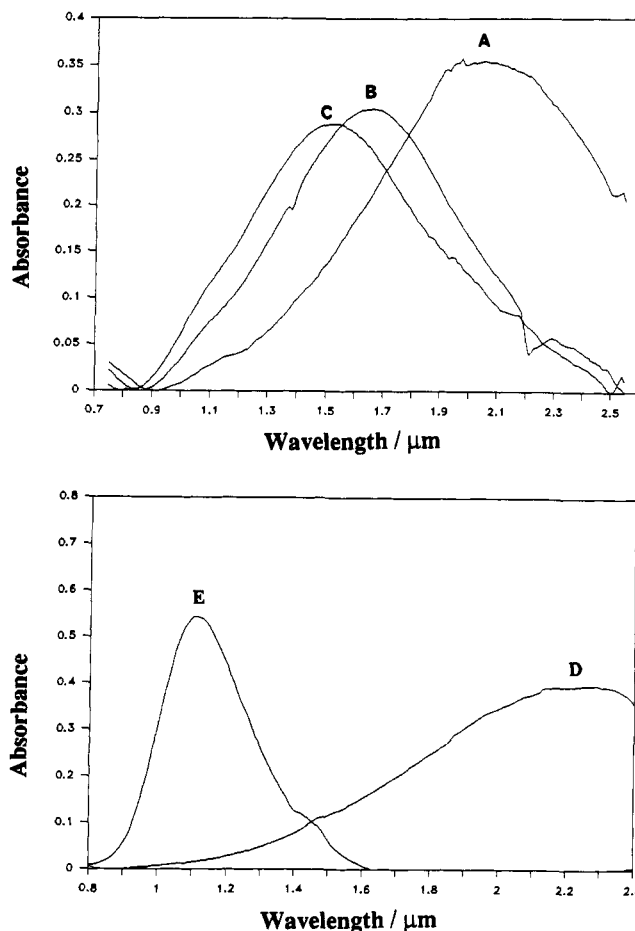


Figure 3. Vis-NIR spectra of  $2^-$ . (A)  $2^-(\text{Py}^+\text{CH}_2\text{Ph})$ , (B)  $2^-(\text{Py}^+\text{Me})$ , (C)  $2^-((\text{CH}_2)_2\text{N}^+\text{Me}_3)$ , (D)  $2^-(\text{H})$  in water; (E)  $2^-(\text{CH}_2\text{CO}_2\text{H})$  in aq pH 7 buffer. All 0.9 mM.

enhanced by added electrolyte and dissipated by less polar, nonaqueous solvents. It has been observed that dye aggregation can give blue shifts of the  $\pi$ - $\pi^*$  band maxima,<sup>7a,b</sup> and this has been theoretically explained in terms of a slipped stack structure and exciton theory.<sup>7c</sup> Without a more extensive discussion that has been provided elsewhere,<sup>10,11</sup> we invoke the same explanation here for shifts in the  $\pi$ - $\pi^*$  bands. Thus, it is found that monomeric  $2^-$  absorbs at about 473 nm, dimeric  $2^-$  at about 451 nm, and stacked  $2^-$  at even shorter wavelengths. Table II shows a clear correlation of longer wavelength NIR with shorter wavelength visible absorptions.

The literature on single-crystal  $\pi$ -stacked salts indicates that mixed valence is important for conductivity, and it is typical that mixed stacks, which include anion radicals and neutrals, are present when good conductivity is observed.<sup>1,5,12</sup> For this reason the effects of varying the extent of reduction have been briefly explored. In the case of  $1^-$  the NIR  $\lambda_{\max}$  did not change as the extent of reduction was varied over the range 0.5–1.5 electrons/molecule. When  $2^-(\text{Py}^+\text{CH}_2\text{Ph})$  was studied, the  $\lambda_{\max}$  was unchanged when less than 1 equiv was used, suggesting that anion radical stacks are responsible for the spectrum reported in Figure 3 and are not perturbed by the mixing in of neutrals. However, when 1.2 electrons/molecule was added, the  $\lambda_{\max}$  shifted to even longer wavelengths (beyond 2500 nm). This is preliminarily interpreted to mean that

(11) Miller, L. L.; Zhong, C. J.; Kasai, P. H. Submitted for publication.

(12) Heywang, G.; Born, L.; Fitzky, H.-G.; Hassel, T.; Hocker, J.; Miller, H.-K.; Pittel, B.; Roth, S. *Angew. Chem., Int. Ed. Engl.* 1989, 28 (4), 483.

mixed stacks of anion radicals and dianions can be formed and that they will be better conductors than if only anion radicals are involved. This may also explain the CV results and will be pursued in more detail in the future.

Better aggregation of the cationically substituted  $2^-$  is reasonable because it should be more favorable coulombically to bring together singly charged "dication/anion-radicals" than triply charged  $1^-$  species. Comparison of the pyridinium and alkylammonium species shows that the rigid, more hydrophobic  $2^-(\text{Py}^+\text{CH}_2\text{Ph})$  anion radical is the best aggregator. We propose by analogy to other amphiphilic aggregation phenomena in water that bringing together the hydrophobic parts of the monomers minimizes the disruption of the water structure but allows van der Waals bonding between the organic molecules. Thus, the larger and rigid *N*-benzylpyridinium groups would have the highest tendency to aggregate. Importantly, these are organized aggregates due to the stabilization resulting from delocalization of the aromatic anion radical electrons along the stack.

The simplest anion radical  $2^-(\text{H})$  formed in aqueous solution with dithionite gave NIR absorption near 2000 nm. This suggests that higher aggregates were formed and, indeed, it was found that precipitation took place so rapidly that it was difficult to get the spectrum. Even more rapid was the precipitation of the anion radical  $2^-(\text{OH})$ . In this case no useful spectra could be recorded. Smaller aggregates and less solubility problems were encountered with  $2^-(\text{OMe})$ , which showed the  $\lambda_{\text{max}}$  for the excitonic absorption at 1291 nm. The pyridine terminated  $2^-(\text{Py})$  showed a NIR band at 1471 nm in pH 10 solution and 1400 nm in pH 7 solution.

As expected from the results for  $1^-$  the four anionic substituted  $2^-$  dimerized in water, instead of forming larger aggregates (Table II). Thus,  $2^-(\text{CH}_2\text{CO}_2\text{H})$ ,  $-((\text{CH}_2)_5\text{CO}_2\text{H})$ ,  $-(\text{CH}_2\text{SO}_3^-)$ , and  $-((\text{CH}_2)_3\text{SO}_3^-)$  all showed a NIR band near 1116 nm and a  $\pi-\pi^*$  band at 450 nm. The carboxylic acids were studied in pH 7 and 10 buffers to ensure deprotonation.

**ESR Spectra.** Spectra were recorded in DMF solution on electrogenerated  $2^-$ . In each case the spectrum showed hyperfine coupling with  $a_{\text{H}} = 1.9$  G (4 naphthyl hydrogens) and  $a_{\text{N}} = 0.85$  G (2 N). The compounds with *N*-alkyl groups showed a further small splitting by four hydrogens with  $a_{\text{H}} = 0.25$  G. Anionically substituted compounds  $2^-(\text{CH}_2\text{SO}_3^-)$ ,  $-((\text{CH}_2)_5\text{SO}_3^-)$ ,  $-(\text{CH}_2\text{CO}_2\text{H})$ , and  $-((\text{CH}_2)_5\text{CO}_2\text{H})$ , which are dimerized in water, show the same hyperfine coupling pattern (Figure 4). By comparison with standards, it was shown that the doubly integrated signal intensity in water for these anionically substituted  $2^-$  is about 5% of that in DMF, and the spectra are thought to arise from a small amount of monomeric  $2^-$ . Those anion radicals with longer wavelength NIR absorption spectra also show weak signals but without hyperfine coupling. In the case of  $2^-$  derivatives with absorption beyond 1400 nm the signals<sup>13</sup> are anisotropic (Figure 4). In this case it is proposed that the larger stacks do not rotate end-to-end rapidly enough to produce isotropic signals. It has been shown that similar anisotropic spectra are also produced in solid powders.<sup>2,3</sup>

### Conclusions

The optical, ESR, and CV data are in agreement that  $\pi$ -dimers and  $\pi$ -stacks are formed from all these anion radicals in aqueous media. Anionically substituted  $2^-$  form

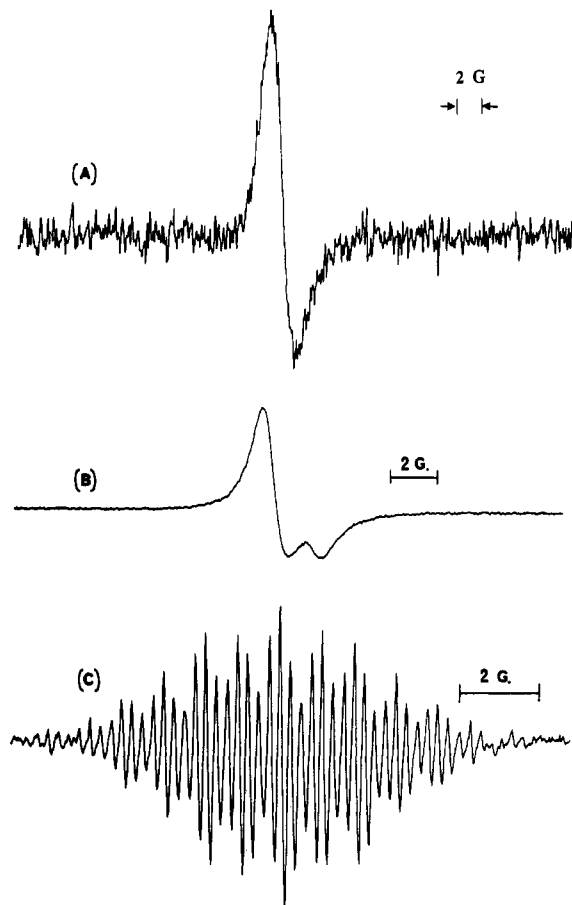


**Figure 4.** ESR spectra in water (1 mM) of (A)  $2^-(\text{Py}^+\text{CH}_2\text{Ph})$ ; (B)  $2^-(\text{Py})$ ; (C)  $2^-(\text{CH}_2\text{CO}_2\text{H})$ . For (A) and (B) modulation amplitude = 1 G; (C) = 0.2 G.

dimers, while cationically terminated  $2^-$  and  $2^-(\text{H})$  form stacks. The results are rational in terms of Coulombic and hydrophobic forces. Important also is the delocalization of electrons along the stack, which is essentially independent of the forces acting on the terminal groups. It is this stack delocalization which gives organization and interesting properties to the aggregates. We note again that  $\pi$ -stacks are central to conducting materials formed from ion radicals. In these solids the excitonic bands usually are found at wavelengths beyond 2000 nm. Thus, we believe that shorter stacks are present in solution than in these solids. Our current work aims to elucidate the stack size in solution and correlate the properties with those in solids. Important in these studies is the effect of added salts or other aggregation agents. It has been shown, for example, that certain salts will shift the NIR exciton band for  $2^-(\text{R} = \text{Py}^+\text{Me})$  well beyond 2500 nm. In contrast the dimerized  $2^-(\text{R} = \text{CH}_2\text{CO}_2^-)$  spectrum is unaffected by added salts.

### Experimental Section

**General Methods.** The following chemicals were purchased from Aldrich Chemical Co. and were used without further purification: 1,4,5,8-naphthalenetetracarboxylic acid dianhydride, 4-aminopyridine, *N,N*-dimethylethylenediamine, *N,N*-dimethylpropylenediamine, benzyl bromide, dimethyl sulfate, *N,N*-dimethylacetamide (DMA) anhydrous (stored over activated 4-Å molecular sieves (MCB)), dimethylformamide (DMF) anhydrous grade, and lithium perchlorate. Phosphate buffer solutions were used.

Infrared spectra were run on a Perkin-Elmer 1600 FT-IR instrument. NMR spectra were obtained with an IBM-AC 200, Varian Unity 300, or Varian Unity 500 spectrometer. Spectra

(13) Wertz, J. E.; Bolton, J. R. *Electron Spin Resonance*; Chapman and Hall: London, 1986; p 131.

are reported in  $\delta$  ppm. Fast-atom bombardment (FAB) mass spectra were recorded on a VG 7070E-HF instrument using *m*-nitrobenzyl alcohol (MNBA) as matrix. UV-visible spectra were run on a Shimadzu 160 spectrometer. HPLC analyses were done using a system composed of two Waters Associates Model 6000A pumps with a Model 660 solvent programmer and a variable-wavelength UV detector manufactured by Applied Biosystems, Model 757. The column was a VYDAC TP 218 C<sub>18</sub> reverse-phase column. NIR spectra were taken using a Cary-170 spectrometer. The absorbance was recorded at 10-nm intervals. Usually 10 data points were averaged for each wavelength. ESR spectra were recorded on a Bruker ESR-300 instrument at 9.7 GHz. The modulation frequency was 100 kHz. A gastight syringe was used to transfer the anion radical solution into a deaerated custom-made quartz tube. Ten to fifteen scans were averaged to yield the final spectrum. For the spin count experiment, the intensity of the signal was doubly integrated and compared to that of a known concentration of TEMPO as the standard. Electrochemical equipment has been described.<sup>2</sup> SCE was used as the reference electrode.

**2(H).** 1,4,5,8-Naphthalenetetracarboxylic acid dianhydride (0.5 g) and ammonium carbonate (2.0 g) were mixed in 50 mL of 30% ammonium hydroxide aqueous solution. After reaction under stirring for 2 h, the mixture was heated to evaporate all the solvent and was further heated to  $\sim 250$  °C for 8 h. Gray-colored powders were obtained. The crude product was washed with H<sub>2</sub>O and ether, dissolved in hot DMSO, and crystallized by adding a small amount of H<sub>2</sub>O. The IR spectrum agreed with the literature.<sup>14</sup> FAB MS (H<sub>3</sub>PO<sub>4</sub> matrix): calcd for C<sub>14</sub>H<sub>6</sub>N<sub>2</sub>O<sub>4</sub> 266.0326, found 267.0409 (M + H<sup>+</sup>).

**2(OH).** Following Schütz et al.<sup>15</sup> 1,4,5,8-naphthalenetetracarboxylic acid dianhydride (2 mmol), hydroxylamine hydrochloride (6 mmol), and sodium carbonate (6 mmol) were mixed in 15 mL of water. The mixture was stirred at 100 °C under reflux for 4 h. After cooling to room temperature, the mixture was filtered and rinsed with water. The violet-black powders were dissolved in 15 mL of water, and at 90 °C 1 N HCl solution was slowly added into it under stirring until pH  $\sim 2$  was reached. A yellowish suspension resulted. It was filtered, washed with water and recrystallized in 3:1 DMF-H<sub>2</sub>O. Yellow flakes were obtained. FTIR (KBr): 1703 and 1663 (imide C=O sym and asym stretching) and other vibrations at 3481, 3421, 3275, 3084, 3047, 2917, 2843, 2672, 1583, 1449, 1419, 1371, 1347, 1251, 1212, 1121, 1005, 980, 898, 755, 740, 670, 573 cm<sup>-1</sup>. The -OH bands are well resolved in the region 3421-3271 cm<sup>-1</sup>. <sup>1</sup>H NMR (200 MHz, DMSO): 8.68 (s, 4 naphthyl H), 11.06 (-OH). FAB MS (MNBA matrix): calcd for C<sub>14</sub>H<sub>6</sub>N<sub>2</sub>O<sub>6</sub> 298.0224, found 299.0327 (M + H<sup>+</sup>).

**2(OMe).** 1,4,5,8-Naphthalenetetracarboxylic acid dianhydride (0.536 g), methoxylamine hydrochloride (0.501 g), and sodium carbonate (0.744 g) were mixed in 15 mL of water. The mixture was refluxed at 80 °C under stirring for 6 h. It was filtered and washed with water. The resulting crude product was recrystallized in 4:1 DMF-H<sub>2</sub>O and washed with ether. A fluffy yellow product was obtained. FTIR (KBr): 1732 and 1687 (imide C=O), and other vibrations at 3447, 3082, 3043, 3004, 2944, 1581, 1508, 1442, 1370, 1334, 1244, 1211, 1121, 1018, 976, 910, 884, 755, 735, 600, 536 cm<sup>-1</sup>. <sup>1</sup>H NMR (200 MHz, DMSO): 8.71 (s, 4 naphthyl H), 4.00 (s, 6 OCH<sub>3</sub> H). FAB MS (MNBA matrix): calcd for C<sub>16</sub>H<sub>10</sub>N<sub>2</sub>O<sub>6</sub> 326.0536, found 327.0635 (M + H<sup>+</sup>).

**2(CH<sub>2</sub>CO<sub>2</sub>H).** 1,4,5,8-Naphthalenetetracarboxylic acid dianhydride (0.54 g), glycine hydrochloride (0.7 g), and sodium carbonate (0.88 g) were mixed in 20 mL of water. It was refluxed at 50 °C under stirring for 5 h. HCl (1 N) was slowly added into the resulting solution until a white suspension resulted (pH  $\sim 2$ ). It was filtered and washed with water. The yellowish crude product was further washed with water. A gray powder was obtained. FTIR (KBr): 1710 and 1671 (imide C=O), and other vibrations at 3432, 3082, 3042, 3002, 2961, 2670, 2585, 1583, 1456, 1398, 1359, 1326, 1248, 1189, 1123, 1009, 900, 810, 775, 726, 710, 612 cm<sup>-1</sup>. The carbonyl band of the carboxylic group is superimposed in the region of the imide carbonyl bands. <sup>1</sup>H NMR (200

MHz, DMSO): 8.76 (s, 4 H), 4.78 (s, 4CH<sub>2</sub>-), 11.5 (-CO<sub>2</sub>H). FAB MS (MNBA matrix): calcd for C<sub>18</sub>H<sub>10</sub>N<sub>2</sub>O<sub>8</sub> 382.0434, found 383.0491 (M + H<sup>+</sup>).

**2((CH<sub>2</sub>)<sub>3</sub>CO<sub>2</sub>H).** 1,4,5,8-Naphthalenetetracarboxylic acid dianhydride (0.54 g) and 5-aminopentanoic acid (0.80 g) were mixed in 15 mL of DMA. It was refluxed at 100 °C under stirring for 4 h. After cooling down, it was filtered and washed with DMA and ether. The crude product was further washed with ether and water. FTIR (KBr): 1706 and 1659 (imide C=O), and other vibrations at 3420, 3087, 2937, 2851, 2670, 2585, 1560, 1457, 1406, 1377, 1340, 1268, 1244, 1161, 1114, 1075, 978, 890, 770, 568 cm<sup>-1</sup>. <sup>1</sup>H NMR (200 MHz, D<sub>2</sub>O + NaOD for solubility): 8.47 (s, 4 naphthyl H), 4.13 (s, 4 N-CH<sub>2</sub>-), 2.21 (4 CH<sub>2</sub>-CO<sub>2</sub>H), and 1.6-1.4 (12 -(CH<sub>2</sub>)<sub>3</sub>-). FAB MS (MNBA matrix): calcd for C<sub>26</sub>H<sub>26</sub>N<sub>2</sub>O<sub>8</sub> 494.1682, found 495.1767 (M + H<sup>+</sup>).

**2(CH<sub>2</sub>SO<sub>3</sub><sup>-</sup>).** Sodium carbonate (0.37 g) and aminomethanesulfonic acid (0.67 g) were dissolved and stirred in a 10 mL of water. It was then dried under vacuum and 100 °C. The resulting aminomethanesulfonate was mixed with 1,4,5,8-naphthalenetetracarboxylic acid dianhydride (0.54 g) in 15 mL of DMA. It was refluxed at 100 °C under stirring for 20 h. After cooling down, it was filtered, and the filtrate was cracked down by ether. The crude product was recrystallized in DMF with ether, and was filtered and washed with ether. A yellow product was obtained. FTIR(KBr): 1717 and 1676 (imide C=O), 1214 (-SO<sub>3</sub><sup>-</sup> stretching), and other vibrations at 3447, 3089, 3046, 2971, 2935, 1582, 1457, 1400, 1352, 1320, 1214, 1172, 1102, 1048, 1000, 890, 763, 559, 524 cm<sup>-1</sup>. <sup>1</sup>H NMR (200 MHz, DMSO): 8.70 (s, 4 naphthyl H), 4.99 (s, 4 CH<sub>2</sub>-). FAB MS (MNBA matrix): calcd for C<sub>18</sub>H<sub>8</sub>N<sub>2</sub>O<sub>10</sub>S<sub>2</sub>Na<sub>2</sub> 497.9414, found 498.9489 (M + H<sup>+</sup>).

**2((CH<sub>2</sub>)<sub>3</sub>SO<sub>3</sub><sup>-</sup>).** 1,4,5,8-Naphthalenetetracarboxylic acid dianhydride (0.268 g) and 3-amino-1-propanesulfonate sodium salt (0.591 g) were mixed in 15 mL of DMA. The reaction conditions and purification were the same as for the preparation of 2-(CH<sub>2</sub>SO<sub>3</sub><sup>-</sup>). FTIR (KBr) 1703 and 1662 (imide C=O, 1191 (-SO<sub>3</sub><sup>-</sup> stretching), and other vibrations at 3466, 3033, 2967, 2926, 2837, 1582, 1458, 1380, 1338, 1267, 1244, 1191, 1110, 1052, 981, 890, 771, 668, 617, 589, 529 cm<sup>-1</sup>. NMR (200 MHz, DMSO): 8.69 (s, 4 naphthyl H), 4.11 (4 N-CH<sub>2</sub>-), 2.51 (4 CH<sub>2</sub>-SO<sub>3</sub>H), 1.96 (4 CH<sub>2</sub>-) FAB MS (MNBA matrix): calcd for C<sub>20</sub>H<sub>16</sub>N<sub>2</sub>O<sub>10</sub>S<sub>2</sub>Na<sub>2</sub> 554.0038, found 555.0107 (M + H<sup>+</sup>).

**2(Py).** 1,4,5,8-Naphthalenetetracarboxylic acid dianhydride, (0.38 mmol, 0.103 g) and 10 mL of DMA were added to a two-necked, 25-mL round-bottom flask. A reflux condenser, fitted with a drying tube containing anhydrous calcium sulfate, was inserted into one neck of the flask. The flask was then purged with nitrogen, and 4-aminopyridine (1.14 mmol, 0.115 g) was added into the mixture. The mixture was then stirred and heated to 140 °C for 24 h. Upon cooling to room temperature, 20 mL of diethyl ether was added to precipitate out the product. This was filtered through a fine porosity glass frit and rinsed with diethyl ether (3 $\times$  10 mL). The diimide (0.1 g, 63%) was obtained as a beige color powder. The crude product was subjected to infrared spectroscopy and checked if full imidization had been achieved.

**2(Py<sup>+</sup>Me).** 2(Py) (0.09 mmol, 40.5 mg) and dimethyl sulfate (90  $\mu$ L, 0.9 mmol) were dissolved in 10 mL of DMA inside a 25-mL round-bottom flask for 24 h. After 1 h, a white precipitate formed. Diethyl ether (20 mL) was added to fully precipitate out the product which was then filtered, washed (3 $\times$ , 10 mL) by diethyl ether and dried. A white powder (52.6 mg, 87%) was obtained. IR (KBr) 3053, 1718, 1677, 1446, 1348, 1250, 1059 cm<sup>-1</sup>. <sup>1</sup>H NMR (D<sub>2</sub>O) 9.10 (4 H, d, *J* = 7.7), 8.89 (4 H, s), 8.23 (4 H, d, *J* = 7.7), 4.54 (6 H, s), 3.71 ppm (6 H, s). FAB MS (MNBA matrix) calculated for C<sub>24</sub>H<sub>18</sub>N<sub>4</sub>O<sub>8</sub>S 450.1324; observed (M<sup>+</sup>) 450.1317. HPLC retention time 3.75 min; flow rate 0.5 mL/min.

**2(Py<sup>+</sup>CH<sub>2</sub>Ph).** The procedure for synthesizing 2(Py<sup>+</sup>Me) was followed except that 31.6 mg (0.074 mmol) of 2(Py) and 88  $\mu$ L (0.74 mmol, 127.1 mg) of benzyl bromide were used. A bright yellow precipitate (39.2 mg, 70%) was collected. IR (KBr) 3025, 2926, 1718, 1676, 1444, 1342, 1247, 1184 cm<sup>-1</sup>. <sup>1</sup>H NMR (D<sub>2</sub>O) 9.19 (4 H, d, *J* = 7.7), 8.87 (4 H, s), 8.24 (4 H, d, *J* = 7.7), 7.56 (10 H, m), 5.97 ppm (4 H, s). FAB MS (MNBA matrix) calculated for C<sub>38</sub>H<sub>28</sub>N<sub>4</sub>O<sub>4</sub> 602.1948, observed (M<sup>+</sup>) 602.1971. HPLC retention time 4.24 min; flow rate 0.5 mL/min.

**2((CH<sub>2</sub>)<sub>2</sub>-N(CH<sub>3</sub>)<sub>2</sub>).** The procedure for making 2(Py) was used except that 0.125 g (0.47 mmol) of anhydride and 120  $\mu$ L (1.4

(14) Pouchert, C. J. *Aldrich Library Infrared Spectra* 1981, 2, 1100A, 1981.

(15) Schütz, V. S.; Kurz, J.; Phimpe, H.; Bock, M.; Otten, H. *Arzneim.-Forsch (Drug Res.)* 1971, 6, 739.

mmol) of *N,N*-dimethylethylenediamine were used instead. Orange yellowish needles (0.15 g, 75%) resulted after ethereal workup.

$2((\text{CH}_2)_2\text{N}^+(\text{Me})_3)$ . The procedure for preparing  $2(\text{Py}^+\text{Me})$  was followed except that 20.9 mg (0.078 mmol) of  $((\text{CH}_2)_2\text{N}(\text{CH}_3)_2)$  and 67  $\mu\text{L}$  (0.78 mmol) of dimethyl sulfate were used. A pale white precipitate (52 mg, 80%) was collected. IR (KBr) 3080, 2949, 2820, 2770, 1702, 1657, 1582, 1455, 1350, 1245, 1160  $\text{cm}^{-1}$ .  $^1\text{H}$  NMR ( $\text{D}_2\text{O}$ ) 8.73 (4 H, s), 4.64 (4 H, t,  $J = 7.7$ ), 3.67 (10 H, m), 3.29 ppm (18 H, br s). FAB MS (MNBA matrix) calculated for  $\text{C}_{24}\text{H}_{30}\text{N}_4\text{O}_4$  438.2260, observed ( $\text{M}^+$ ) 438.2257. HPLC retention time 3.53 min; flow rate 0.5 mL/min.

$2((\text{CH}_2)_3\text{N}(\text{CH}_3)_2)$ . The procedure for  $2(\text{Py})$  was used except that 0.101 g (0.38 mmol) of anhydride and 142  $\mu\text{L}$  (1.13 mmol)

of *N,N*-dimethylpropylenediamine were used instead. A bright yellowish powder (0.09 g, 54%) was isolated after workup.

$2((\text{CH}_2)_3\text{N}^+(\text{Me})_3)$ . The procedure for preparing  $2(\text{Py}^+\text{CH}_3)$  was followed except that 48.7 mg (0.1 mmol) of  $2((\text{CH}_2)_3\text{N}(\text{CH}_3)_2)$  and 106  $\mu\text{L}$  (1.1 mmol) of dimethyl sulfate were used. A pale white precipitate (48 mg, 70%) was collected. IR (KBr) 2975, 2944, 2814, 2779, 2759, 1698, 1653, 1454, 1345, 1254, 1242, 1041  $\text{cm}^{-1}$ .  $^1\text{H}$  NMR ( $\text{D}_2\text{O}$ ) 8.63 (4 H, s), 4.23 (4 H, t,  $J = 7.7$ ), 3.68 (6 H, m), 3.51 (4 H, t,  $J = 7.7$ ), 3.12 (18 H, br s), 2.26 (4 H, m). FAB MS (MNBA matrix) calculated for  $\text{C}_{26}\text{H}_{34}\text{N}_4\text{O}_4$  466.2572, observed ( $\text{M}^+$ ) 466.2591. HPLC retention time 3.58 min; flow rate 0.5 mL/min.

**Acknowledgment.** This work was supported by NSF and ONR.

## Thin-Film Indium Selenide Prepared by Reaction of Selenium Vapor with Indium Oxide

Shixing Weng, Henry Wynands, and Michael Cocivera\*

Guelph-Waterloo Centre for Graduate Work in Chemistry, University of Guelph, Guelph, Ontario, Canada N1G 2W1

Received July 16, 1992. Revised Manuscript Received September 28, 1992

A new process involving two steps has been developed to prepare thin-film  $\text{In}_2\text{Se}_3$ . The first step is formation of indium oxide by spray pyrolysis of an aqueous solution of indium nitrate, and the second is reaction of this oxide with selenium vapor in nitrogen at atmospheric pressure to form  $\text{In}_2\text{Se}_3$ . Shorter exposure time was needed for complete conversion as the temperature was increased from 400 to 500  $^\circ\text{C}$ . Auger depth profiling of the composition of a partially converted film indicated that the conversion process appears to involve three steps: (a) reaction between selenium vapor and the oxide at the surface; (b) subsequent diffusion of selenium into the film until much of the oxide was converted to InSe; (c) further reaction involving selenium vapor and InSe to form  $\text{In}_2\text{Se}_3$ . It was possible to convert  $\text{In}_2\text{Se}_3$  into InSe by reacting it with indium vapor, and it was also possible to incorporate cadmium. p-type  $\text{In}_2\text{Se}_3$  and n-type InSe were prepared by this relatively inexpensive process. Resistance and Hall effect measurements gave a variety of resistivity and carrier density values, depending on the preparation conditions. X-ray diffraction indicated that the  $\text{In}_2\text{Se}_3$  film may consist of several crystalline phases, and optical absorption spectra indicated a direct bandgap of 1.84 eV. A direct bandgap of 3.64 eV was found for  $\text{In}_2\text{O}_3$ , which was n-type and had a very low resistivity and high electron density.

### Introduction

There has been a recent interest in the growth of thin films of  $\text{In}_2\text{Se}_3$  for a variety of applications.<sup>1-3</sup> The complex hexagonal layered structure of this material makes it possible for ions to diffuse in and alter the physical properties without changing the structure.<sup>4,5</sup> This behavior permits the use of this material as a cathode in microbatteries and as solid solution electrodes in microcapacitors.<sup>6</sup> The bandgap and other properties of this material also make it attractive for solar energy conversion.<sup>7-11</sup> Various methods have been used to prepare thin-film indium selenide including elemental evaporation,<sup>12,13</sup> molecular beam epitaxial growth,<sup>14</sup> electrodeposition,<sup>15</sup> and evaporation of indium selenide powder.<sup>16</sup> In the present paper, we report a new process for preparing indium selenide, which employs two steps that do not require the use of expensive equipment. The first step involves the use of spray pyrolysis to prepare thin-film  $\text{In}_2\text{O}_3$ , and the second step involves the formation of  $\text{In}_2\text{Se}_3$  by reaction of elemental selenium vapor with the indium oxide film at atmospheric pressure in a nitrogen ambient. Some of the preparation parameters are explored to determine the effects on film composition and the extent of

the conversion. In addition preliminary results are presented for the structural, electrical and optical properties

- (1) Julien, C.; Eddried, M.; Kambas, K.; Balkanski, M. *Thin Solid Films* 1986, 137, 27.
- (2) Watanabe, I.; Yamamoto, T. *Jpn. J. Appl. Phys.* 1985, 24, 1282.
- (3) Yudasada, M.; Nakanishi, K. *Thin Solid Films* 1988, 156, 145.
- (4) Samaras, I.; Tsakiri, M.; Julien, C. In *Chemical Physics of Intercalation*; Legrand, P. A., Flandrois, S., Eds.; NATO ASI Series; Plenum Press: New York, 1987.
- (5) Whittingham, M. S. *Prog. Solid State Chem.* 1978, 12, 41.
- (6) Balkanski, M. *Appl. Surf. Sci.* 1988, 33/34, 1260.
- (7) Segura, A.; Guesdon, J. P.; Besson, J. M.; Chevy, A. *Rev. Phys. Appl.* 1979, 14, 253.
- (8) Di Giulio, M.; Micocci, G.; Rizzo, A.; Tepore, A. *J. Appl. Phys.* 1983, 54, 5839.
- (9) Martinez-Pastor, J.; Segura, A.; Valdes, J. L.; Chevy, W. *J. Appl. Phys.* 1987, 62, 1477.
- (10) Levy-Clement, C.; Le Nagard, N.; Gorochoy, O.; Chevy, A. *J. Electrochem. Soc.* 1984, 131, 790.
- (11) Tenne, R.; Theys, B.; Rioux, J.; Levy-Clement, C. *J. Appl. Phys.* 1985, 57, 141.
- (12) Thomas, B. *Appl. Phys. A* 1992, 54, 293.
- (13) Watanabe, Y.; Kaneko, S.; Kawazoe, H.; Yamane, M. *Phys. Rev. B* 1989, 40, 3133.
- (14) Emery, J. Y.; Brahim-Ostmane, L.; Hirlimann, C.; Chevy, A. *J. Appl. Phys.* 1992, 71, 3256.
- (15) Sanheeviraja, C.; Mahalingam, T. *J. Mater. Sci. Lett.* 1992, 11, 525.
- (16) Kenawy, M. A.; Zayed, H. A.; Abo El-Soud, A. M. *J. Mater. Sci. Mater. Elect.* 1990, 1, 115.

\* To whom correspondence should be addressed.